PCCP

PAPER

View Article Online
View Journal | View Issue

Cite this: *Phys. Chem. Chem. Phys.*, 2024, **26**, 18683

Photoswitchable luminescent lanthanide complexes controlled and interrogated by four orthogonal wavelengths of light†

Charlie H. Simms, [a] Villads R. M. Nielsen, [b] Thomas Just Sørensen, [b] Stephen Faulkner *[a] and Matthew J. Langton *[a]

Received 31st May 2024,
Accepted 15th June 2024

DOI: 10.1039/d4cp02243b

rsc.li/pccp

Optical information storage requires careful control of excitation and emission wavelengths in a reversible and orthogonal manner to enable efficient reading, writing, and erasing of information. Photochromic systems, in which a photoswitch is typcially coupled to an emissive organic fluorophore, have much promise in this regard. However, these suffer from considerable spectral overlap between the switch and fluorophore, such that their emissive and photoswitchable properties are not orthogonal. Here, we overcome this limitation by coupling visible/NIR emissive lanthanide complexes with molecular photoswitches, enabling reversible and orthogonal photoswitching with visible light. Crucially, photoswitching does not lead to sensitised emission from the lanthanide, while excitation of the lanthanide does not induce photoswitching, enabling the state of the system to be probed without perturbation of the switch. This opens up the possibility of developing multi-colour read–write methods for information storage using emissive photoswitches.

Introduction

The development of photoresponsive molecular systems is an area of intense current research.[1–5] The ability to engineer spatio-temporal control over molecular function has led to the development of a wide range of molecular photoswitches,[6–8] with applications spanning chemistry,[9] materials science,[10] biology,[11] medicine,[12] and information storage.[13] Azobenzenes are a well-established class of molecular photoswitches, undergoing facile photoisomerisation between *cis* (*Z*) and *trans* (*E*) isomers, with an accompanying change in geometry and dipole moment.[14,15] As a result, many biological applications dependent on the photoisomerisation of azobenzenes have been developed.[16–27] The development of systems which respond to visible and near-infrared (NIR) light are especially desirable as the energy required as a stimulus is much lower in energy in contrast to more typical UV-triggered photoswitches.[28] Photoswitchable emissive derivatives, accessed by coupling an emissive moiety to a molecular photoswitch, are particularly attractive for both the control and interrogation of such systems, particularly for optical information storage in which light is used to "read" and "write" data.[29] In this approach, one wavelength of light is required to "write" the optical information by changing the systems state *via* a photochemical process. Irradiation with a second wavelength of light allows for this optical information to be "read", by probing the state of the system. For effective, reversible read and write steps, these processes must be orthogonal and reversible: *i.e.* the excitation wavelength of the reporter in the "read" step does not perturb the system state (the photochromic reaction); emission does not induce energy transfer to the switch; and that the writing process does not itself lead to emission.[30] Reversibility of the system allows for data erasure and subsequent re-writing (Fig. 1).

In principle, this process could be achieved by independently controlling the molecular switch, whilst using the emission as a read-out of the system's state, provided that the wavelengths of light used to control the photoisomerisation of the switch and the excitation/emission of the chromophore are orthogonal. While organic fluorophores are commonly utilised in imaging applications, the absorbance bands of organic photoswitches and fluorophores often overlap, as a result reading the data without perturbing the system's state (point III) in (Fig. 1) is difficult to achieve.[31] One solution to this challenge is to employ lanthanide complexes as the emissive moiety, with a judicious choice of ligand enabling its decoupling from the lanthanide luminescence.[32] Furthermore, the narrow bandwidth of lanthanide emission also allows for insight into molecular structure,[33] while long emission lifetimes may be exploited in time gated imaging.[34–37]

[a] *Department of Chemistry, University of Oxford Chemistry Research Laboratory, Mansfield road, Oxford, OX1 3TA, UK. E-mail: stephen.faulkner@chem.ox.ac.uk, matthew.langton@chem.ox.ac.uk*
[b] *Nano-Science Centre and Department of Chemistry University of Copenhagen Universitetsparken 5, 2100 København Ø, Denmark*

† Electronic supplementary information (ESI) available. See DOI: https://doi.org/10.1039/d4cp02243b

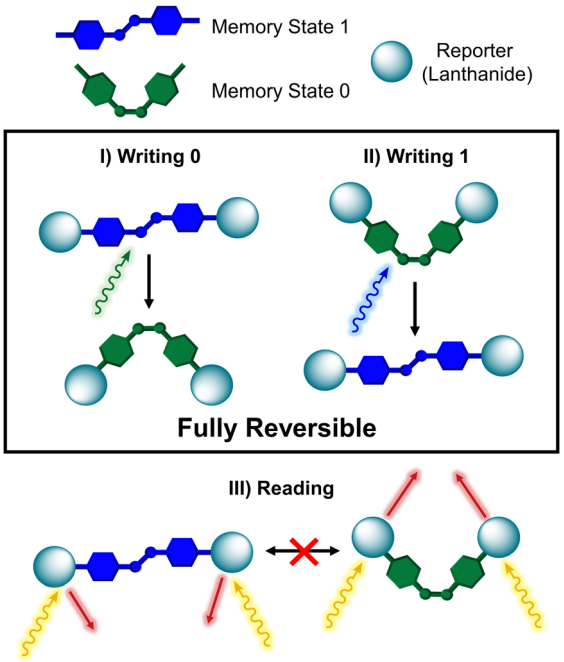

Fig. 1 Design of an optical information storage system, where two azobenzene based memory states can be written by orthogonal wavelengths of light in a fully reversible manner, steps (I) and (II). Step (III) describes the reading of this optical data *via* orthogonal emission of a lanthanide, which itself does not perturb the system state.

Lanthanide complexes with integrated molecular photoswitches are extremely rare. A number of lanthanide dithienylethene complexes have been reported, in which there is considerable spectral overlap between the lanthanide and the photoswitch. Consequently, irradiation into the absorbance band of each isomer directly influences the optical properties of the lanthanides.[38–42] In one report, Kawai and co-workers were able to decouple this system for applications in biological media and optical memory information storage.[30] Conversely, only a handful of azobenzene lanthanide complexes have been previously reported.[43–46] However, there are only two reports of kinetically stable[47] photoswitchable lanthanide complexes, and in these systems the azobenzene moieties have not been optimised, exhibiting inefficient photoisomerisation upon excitation with UV light, and a short thermal half-life for the *Z* isomer.[48,49]

Herein, we report the design and synthesis of photoswitchable lanthanide complexes, with high visible light induced photoswitching efficiency and visible/NIR emission. Importantly, we demonstrate that the excitation and emission of the lanthanide is orthogonal and entirely decoupled from the molecular switch. To the best of our knowledge, this represents the first example of a visible light switchable lanthanide complex in which orthogonal control and interrogation of the system is achieved using an unprecedented four orthogonal wavelengths of visible and NIR light.

Approach

To achieve orthogonal photocontrol, in which photoswitching is decoupled from the excitation and emission of the lanthanide, the choice of both the organic photoswitch and the emissive lanthanide was carefully considered. We identified europium(III) and neodymium(III) as suitable lanthanides, bound within kinetically stable 1,4,7,10-tetraazacyclododecane-1,4,7-tris-*t*-butyl acetate (DO3A) complexes.[50,51] Europium(III) has relatively high quantum yields, long luminescent lifetimes (ms) and emits in the red region, making it easy to detect using conventional spectrometers or fluorescence microscopes.[52–55] However, it has a low molar absorption coefficient and absorbs in the UV/blue region, which can result in unwanted spectral overlap with organic ligands and an increased likelihood of back energy transfer.[56] Therefore, we also targeted analogous neodymium(III) complexes, which have higher molar absorption coefficients and absorb light across a wider range of UV, visible and NIR wavelengths,[57,58] albeit with shorter (ns) luminescent lifetimes and low quantum yields.[58,59] Furthermore, the low-lying excited states of Nd(III) inhibit back energy transfer.[33] We identified *ortho*-fluoroazobenzene as a suitable molecular photoswitch. *Ortho*-heteroatom substitution of azobenzene derivatives is an established method for tuning the orbital energies of each isomer, and hence the switching wavelengths and thermal half-life of the *Z* isomer.[60–62] In the *Z* isomer, the repulsive interactions between the nitrogen lone pairs and the *ortho* substituents destabilise the n orbital and thus red-shift the $S_0 \rightarrow S_1$ ($n \rightarrow \pi^*$) transition, enabling visible light to be used to control the photochemical isomerisation.[63,64] This destabilisation is reduced in the *E* isomer, therefore the separation between the $S_0 \rightarrow S_1$ transitions of the isomers, is enhanced and improved photostationary state (PSS) distributions can be achieved. Notably, the introduction of fluorine in the *ortho* positions of the azobenzene also lowers the energy of the n orbital, stabilising the *Z* isomer and allowing for thermal half-lives of up to 2 years to be achieved.[60,61,65]

The photoswitchable lanthanide complexes prepared and studied in this work are shown in Fig. 2. The tetra-*ortho*-fluoroazobenzene is efficiently photoisomerised using orthogonal visible light wavelengths of 405 nm ($Z \rightarrow E$) and 530 nm ($E \rightarrow Z$). The Eu(III) and Nd(III) complexes are directly excited with violet light and yellow light, respectively, resulting in the emission of red light from europium(III) and NIR light from neodymium(III).

Results and discussion

Synthesis

The synthetic route to access each complex is shown in Scheme 1, with full experimental details and characterisation data available in the ESI.† The asymmetric azo-derivative **4a** was prepared *via* the Mills reaction, in which the nitroso derivative is formed *in situ* from the corresponding aniline and subsequently reacted with **3**.[66] The symmetric azo-derivative **4b** was prepared *via* oxidative dimerisation of **3**.[61] The corresponding alcohol derivatives were accessed by acid-mediated hydrolysis, which were then converted to the tosylates **6a** and **6b**. Reaction with the *tert*-butyl ester derivative of DO3A afforded **7a** and **7b**, which were subsequently deprotected to yield free carboxylic acid groups on the macrocycles, $\mathbf{L_a}$ and $\mathbf{L_b}$, respectively. Finally, the lanthanide coordination by the macrocyclic framework was

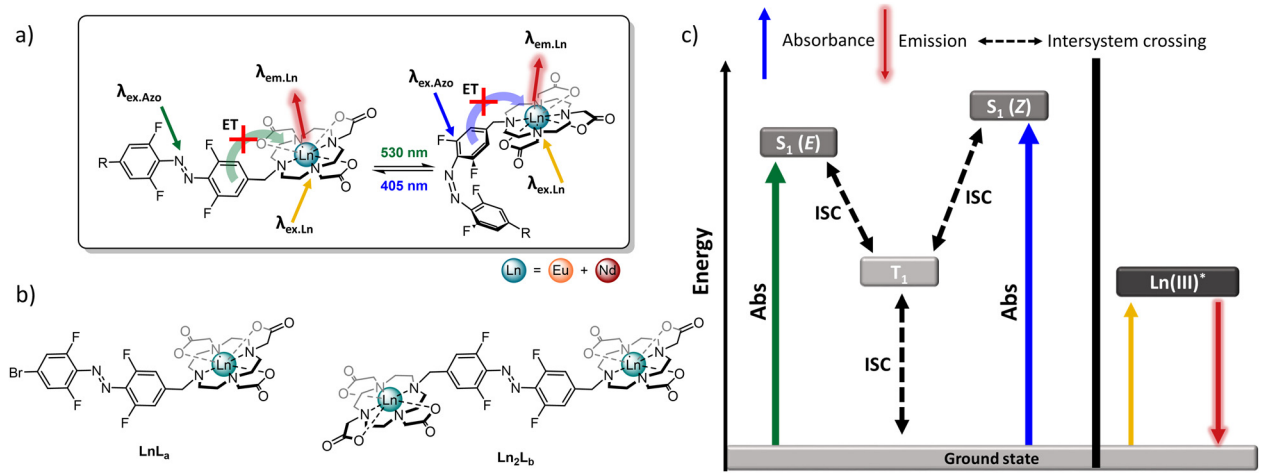

Fig. 2 (a) Schematic representation of orthogonal photoswitching of an azobenzene–lanthanide emissive complex. A tetra-*ortho*-fluoro substituted azobenzene, coupled with a kinetically stable DO3A lanthanide complex, enables orthogonal control over azobenzene photoswitching and the excitation/emission of the lanthanide. (b) Chemical structures of the complexes synthesised **LnL$_a$** and **Ln$_2$L$_b$**, where Ln = Eu(III) or Nd(III). (c) Diagram highlighting the desirable decoupling of photoswitching from Ln(III) emisison within the same complex.

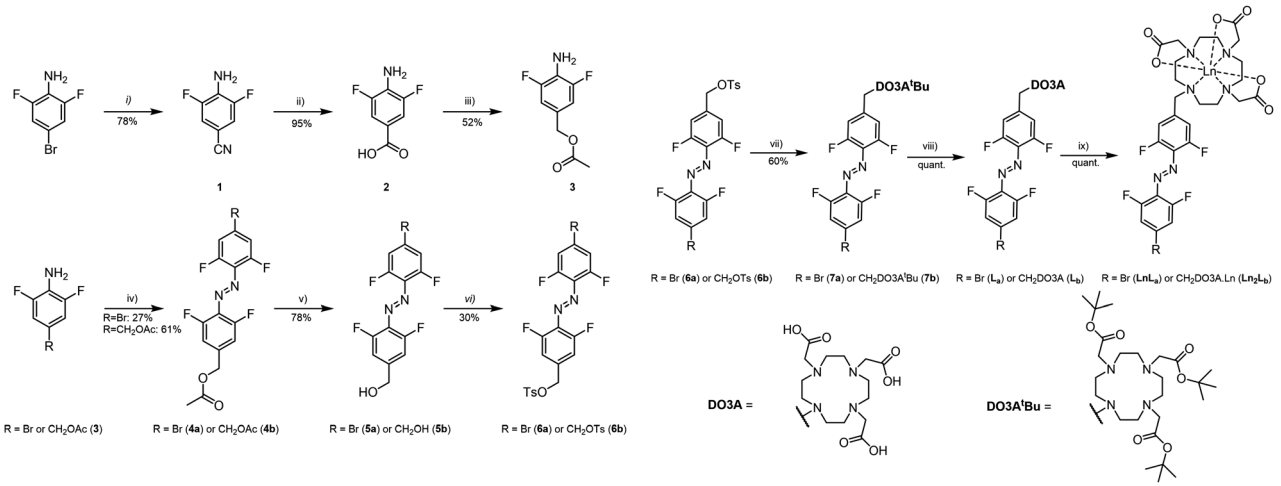

Scheme 1 Synthetic scheme for the synthesis of **LnL$_a$** and **Ln$_2$L$_b$** (i) copper cyanide, *N*-methyl -2-pyrrolidone, 202 °C, 90 minutes, microwave radiation. (ii) potassium hydroxide (30%), 100 °C, 12 hours, (iii) (1) lithium aluminum hydride, tetrahydrofuran, 60 °C, 12 hours; (2) acetic anhydride, pyridine, 25 °C, 12 hours. (iv) for R = Br: oxone, dichloromethane: acetone, 25 °C, 12 hours; if R = CH_2OAc: *N*-chlorosuccinimide, DBU, dichloromethane, −78 °C, 10 minutes. (v) Hydrochloric acid (37%) in methanol, 40 °C, 72 hours. (vi) *p*-tosyl chloride, tetrahydrofuran: water, sodium hydroxide 25 °C, 30 minutes. (vii) DO3A^{t}Bu, acetonitrile, sodium carbonate, 70 °C, 12 hours. (viii) Trifluoroacetic acid, dichloromethane, 25 °C, 12 hours. (ix) Ln(OTf)$_3$, ethanol: water, 50 °C, 72 hours.

achieved by stirring with the appropriate triflate salt, to yield complexes **EuL$_a$**, **Eu$_2$L$_b$**, **NdL$_a$** and **Nd$_2$L$_b$**.

Photoswitching experiments

Photostationary state (PSS) distributions for each ligand following irradiation at 405 and 530 nm for 10 minutes were determined by HPLC analysis (see ESI† for details). Irradiation with blue light from a LED (405 nm, ∼0.9 W) selectively excites the $S_0 \rightarrow S_1$ transition of the *Z* isomers of **LnL$_a$** and **LnL$_b$**, generating an *E*-enriched PSS (up to 91% *E*, Fig. 3). Conversely, irradiation of **LnL$_a$** and **LnL$_b$** with green light using an LED (530 nm, ∼1.1 W), selectively excites into the $S_0 \rightarrow S_1$ transition of the *E* isomer, producing a *Z*-enriched PSS (up to 87% *Z*, Fig. 3).

In agreement with similar *ortho*-fluoro substituted azobenzenes, we observed significant red-shifting of the $S_0 \rightarrow S_1$ ($n \rightarrow \pi^*$) transition, and increased separation between the $S_0 \rightarrow S_1$ transition of the *E* and *Z* isomers compared with unsubstituted azobenzene derivatives.[60] This separation allows for efficient switching using visible light in both directions (absorption spectra of all complexes are available in ESI†).[60,61,67] Notably, the presence of the bulky lanthanide–DO3A complex in the *para* position of the *ortho*-fluoro substituted azobenzene does *not* significantly affect the PSS compared to the analogous *p*-methylene *ortho*-fluoro substituted azobenzene derivative (PSS_{405}:95% *E*, PSS_{530}:84% *Z*),[17] perhaps due to flexibility around the methylene bridge. Additionally, there is negligible change in the absorbance spectra

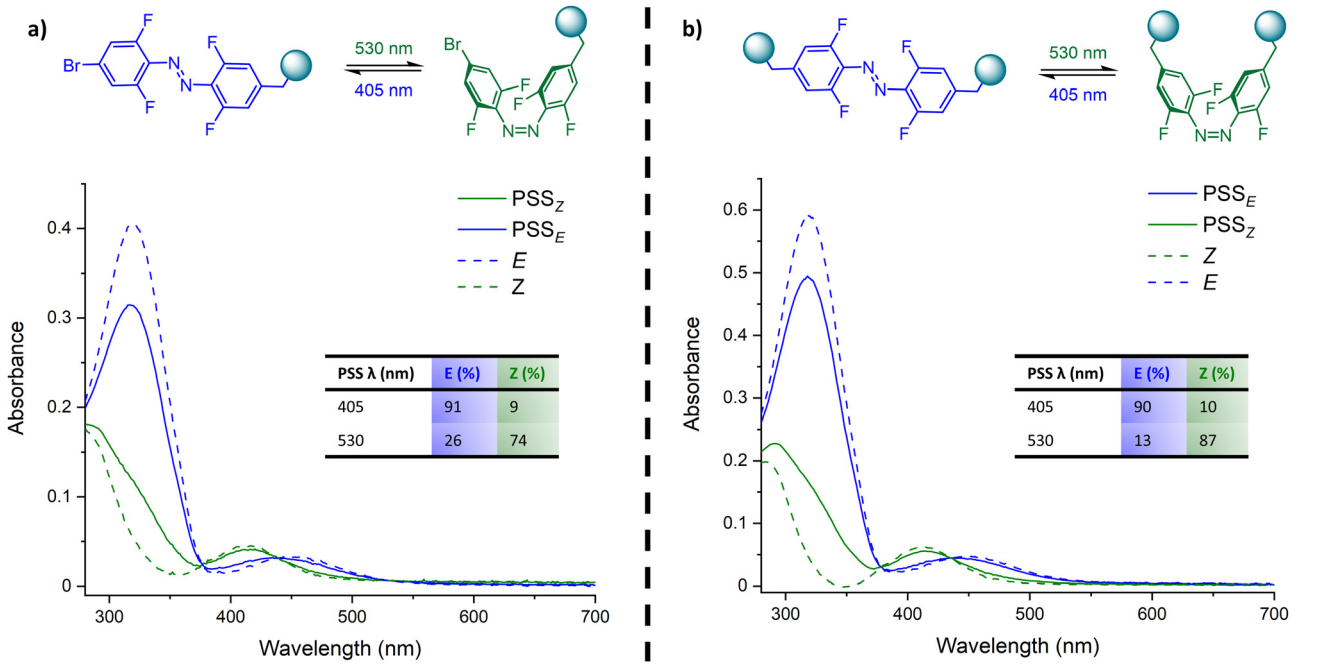

Fig. 3 (a) Absorption spectra of **EuL$_a$** *E* isomer-rich PSS (blue line), calculated pure *E*-isomer of **EuL$_a$** (dashed blue line), **EuL$_a$** *Z*-isomer-rich PSS (green line), calculated pure *Z*-isomer of **EuL$_a$** (dashed green line). Inset: Table of PSS ratios for irradiation with both 405 and 530 nm. (b) Absorption spectra for **Eu$_2$L$_b$** *E*-isomer-rich PSS (blue line), calculated pure *E*-isomer of **Eu$_2$L$_b$** (dashed blue line), **Eu$_2$L$_b$** *Z*-isomer-rich PSS (green line), calculated pure *Z* isomer of **Eu$_2$L$_b$** (dashed green line). Inset: Table of PSS ratios for irradiation with both 405 and 530 nm. Absorption spectra measured in DMSO, upon irradiation for 10 minutes with either 405 nm or 530 nm light. Pure *E* and *Z* isomer spectra were calculated from the spectra of the PSS mixture of known composition (see ESI† for details).

of the ligands **L$_a$** and **L$_b$** upon the chelation of either Eu(III) or Nd(III), suggesting that the π→π* and n→π* transitions are not influenced by the presence of Ln(III) ions in these complexes (Fig. S43, ESI†).

Photophysical behaviour of Eu(III) complexes

Excitation directly into the $^4F_0 \rightarrow {}^5L_6$, transition ($\lambda_{ex}$ = 393 nm) of the *E* and *Z* isomers of the europium(III) complexes **EuL$_a$** and **Eu$_2$L$_b$** afforded red light emission from the Eu(III) metal centre corresponding to the $^5D_0 \rightarrow {}^7F_J$ (J = 0, 1, 2, 3, 4) transitions (Fig. 3a, c and e). Cooling the complexes to 77 K resolved the fine structure in spectra arising from the crystal field splitting of the $^5D_0 \rightarrow {}^7F_J$ (J = 0, 1, 2, 3, 4) transitions (Fig. S44, S45, S48 and S49, ESI†). Excitation spectra were recorded for each Eu(III) complex by monitoring the emission intensity at 616 nm ($^5D_0 \rightarrow {}^7F_2$), the most intense electronic transition. The excitation spectra for both **EuL$_a$** and **Eu$_2$L$_b$** exclusively feature absorption into the excited energy states of Eu(III) corresponding to the $^7F_0 \rightarrow {}^5D_4$, $^5L_{7,8,9}$, $^5L_6$, $^5D_2$, $^5D_1$ transitions. Notably, we observed negligible contribution to Eu(III) emission (λ_{em} = 616 nm) *via* excitation into the azobenzene core (Fig. 4a, b and d). The lack of energy transfer (antenna effect) is attributed to dominating non-radiative decay pathways available *via* the azobenzene core (Fig. 5).[68]

To investigate these effects further, we recorded the emission spectra of the metal-free ligands **L$_a$** and **L$_b$** ($\lambda_{ex(E)}$ = 325 nm ($S_0 \rightarrow S_2$), $\lambda_{ex(Z)}$ = 280 nm ($S_0 \rightarrow S_2$)). The azobenzene-centred emission displayed a characteristic Stokes shift, where the position of the maximum emission wavelength is dependent on the distribution of *E*/*Z* isomers present in solution (Fig. S63–S66, ESI†).[70] Additionally, the intensity of **L$_a$** and **L$_b$** emission was extremely weak, to the extent that direct excitation into the peak of the $S_0 \rightarrow S_1$ transition revealed no detectable emission.[68] This is in concordance with the previously determined extremely low fluorescence quantum yields for both *E*-azobenzene (7.54×10^{-7} to 1.1×10^{-5}, S_1 state) and *Z*-Azobenzene ($\sim 1 \times 10^{-6}$, S_1 state).[71,72] Additionally we observed a change in the absorbance spectra, after excitation into $S_0 \rightarrow S_2$ and $S_0 \rightarrow S_1$ transitions for both isomers of **L$_a$** and **L$_b$**, corresponding to a change in *E*/*Z* isomer composition of the sample (Fig. S63–S66, ESI†).[70,73–75] This is a direct result of the photoisomerisation of the azobenzene. The tendency of **L$_a$** and **L$_b$** to photoisomerise rather than fluoresce suggests that the majority of the energy absorbed is dissipated *via* the non-radiative pathways (Fig. 4).

To investigate the impact of isomerisation upon the photophysical properties of Eu(III) complexes, the excitation and emission spectra of each isomer were compared. Both the excitation and emission spectra of **EuL$_a$** (Fig. 4b and c) and **Eu$_2$L$_b$** (Fig. 4d and e) at 298 K were not perturbed by photoisomerisation of the azobenzene, suggesting that the change in geometry upon isomerisation has minimal impact on the crystal field of Eu(III) in each pair of complexes. Additionally, the Eu(III) lifetimes of both isomers of **EuL$_a$** and **Eu$_2$L$_b$** were measured by fitting the decay of the emission upon excitation at 616 nm (Table 1). Data recorded at 298 K were fitted to a mono-exponential decay, and the negligible difference between the lifetimes of each isomer indicates that the photoisomerisation

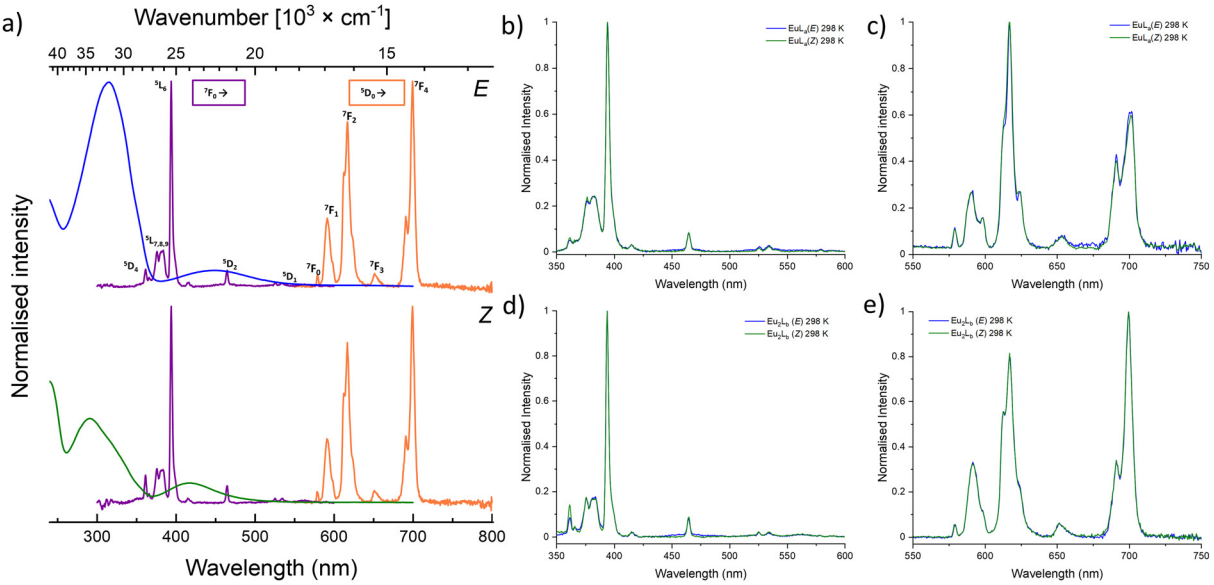

Fig. 4 (a) Stacked normalised spectra of **Eu_2L_b** (*E*) (above), and **Eu_2L_b** (*Z*) (below), with absorbance in blue (*E*) and green (*Z*), excitation spectra in purple and emission spectra in orange at 298 K. (b) Comparison of excitation spectra of **EuL_a** (*E*) (blue) and **EuL_a** (*Z*) (green) at 298 K. (c) Comparison of emission spectra of **EuL_a** (*E*) (blue) and **EuL_a** (*Z*) (green) at 298 K (d) Comparison of excitation spectra of **Eu_2L_b** (*E*) (blue) and **Eu_2L_b** (*Z*) (green) at 298 K. (e) Comparison of emission spectra of **Eu_2L_b** (*E*) (blue) and **Eu_2L_b** (*Z*) (green) at 298 K. Excitation spectra were recorded with λ_{em} = 616 nm, excitation slits 1 nm, emission slit 5 nm, integration time 0.2 s. Emission spectra were recorded with λ_{ex} = 393 nm, emission slits 1 nm, excitation slit 5 nm, integration time 0.2 s. All spectra recorded in DMSO.

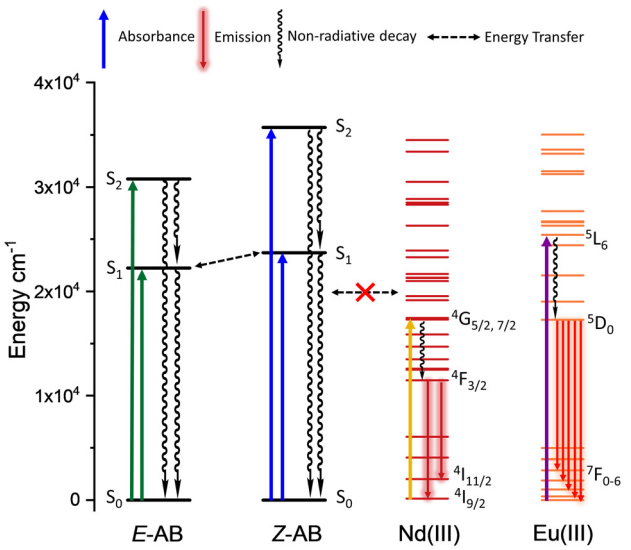

Fig. 5 Jablonski diagram representing the energy levels of both the azobenzene and lanthanide components of the system. The azobenzene *E* and Z isomers can rapidly interconvert between each other upon excitation into both the S_2 and S_1 states, but cannot transfer energy into the excited states of Nd(III) and Eu(III) in **NdL_a**, **EuL_a**, **Nd_2L_b** and **Eu_2L_b** (as measured by Carnall *et al.*[33,69]).

process does not impact the lifetime of the Eu(III) emission. However, at 77 K a bi-exponential decay was required to adequately fit the emission decay profile (Fig. S47 and S51, ESI†), suggesting that at low temperature there are two species present. This is consistent with slow exchange between the twisted square antiprismatic (TSAP) and square antiprismatic (SAP) isomers of the DO3A ligands, which are otherwise in fast exchange at 298 K, resulting in a solution state lifetime representing a weighted average of both isomers.[76–78] The most intense band in the Eu(III) absorption spectrum, the $^4F_0 \rightarrow {}^5L_6$ band (λ_{ex} = 393 nm), lies almost directly between the $S_0 \rightarrow S_2$ and $S_0 \rightarrow S_1$ transitions of the *E*/*Z* isomers of the ligand (Fig. 4a). Upon excitation into the $^4F_0 \rightarrow {}^5L_6$ band (λ_{ex} =393 nm) we observe small perturbations in the PSS distribution (PSS_E = 4% reduction in *E* isomer, PPS_Z = 2% reduction in *Z* isomer) (Fig. S54, ESI†). This is a result of slight overlap between the absorbance of the azobenzene with the $^4F_0 \rightarrow {}^5L_6$ multiplet.

Overall these experiments demonstrate that inducing a large geometric and electronic change to the ligand *via* reversible photoisomerisation has no impact on the photophysics of the emissive Eu(III) metal centre within the same complex.

Photophysical behaviour of the Nd (III) complexes

The data obtained with the Eu(III) complexes demonstrates that the azobenzene ligand plays no role in exciting the lanthanide. Suggesting that, with optimisation, the distinct energy levels of

Table 1 Luminescence lifetimes (τ) of **EuL_a** and **Eu_2L_b** isomers at 298 K and 77 K (λ_{ex} = 395 nm, λ_{em} = 616 nm, 5 nm excitation and emission slits, delay time = 10 ms)

		τ (298 K) (ms)	τ_1 (77 K) (ms)	τ_2 (77 K) (ms)
EuL_a	*E*	1.15	0.21	0.77
	Z	1.34	0.55	—
Eu_2L_b	*E*	1.51	0.34	1.18
	Z	1.48	0.31	0.95

lanthanide(III) ions may be exploited to develop a system in which the direct excitation of the Ln(III) is completely decoupled from the absorbance of the ligand, and does not perturb the PSS of the switch. Therefore, we subsequently examined the spectroscopy and orthogonal switching capabilities of the corresponding Nd(III) complexes. As a result of the lower lying excited states of Nd(III) compared with Eu(III), direct excitation into the Nd(III) metal centre can be achieved by exciting into bands ranging from 500 nm to as far as 900 nm ($^4I_{9/2} \rightarrow {}^4F_{3/2}$, $^2H_{9/2}$, Fig. 6, yellow spectrum). Importantly, this considerably shifts λ_{ex} of Nd(III) away from the region in which the *E*/*Z* isomers of the azobenzene absorb. The corresponding Nd(III) emissions occur at ~880 nm ($^4F_{3/2} \rightarrow {}^4I_{9/2}$), ~1060 nm ($^4F_{3/2} \rightarrow {}^4I_{11/2}$), ~1340 nm ($^4F_{3/2} \rightarrow {}^4I_{13/2}$) and ~1850 nm ($^4F_{3/2} \rightarrow {}^4I_{15/2}$), significantly into the near-IR region.[57,59,79]

Upon excitation into the $^4I_{9/2} \rightarrow {}^4G_{5/2}$, $^2G_{7/2}$ (λ_{ex} = 580 nm) bands of the *E*/*Z* isomers of **NdL$_a$** and **Nd$_2$L$_b$** in solution at 298 K, emission was observed in the near-IR region corresponding to the $^4F_{3/2} \rightarrow {}^4I_{9/2}$ (~880 nm) and $^4F_{3/2} \rightarrow {}^4I_{11/2}$ (~1060 nm) bands (Fig. 6a, c and e). Fine structure in the emission spectra could be resolved when recorded at 77 K (Fig. S55, S56, S58 and S59, ESI†). Similar to **EuL$_a$** and **Eu$_2$L$_b$**, the emission spectra of the *E* and *Z* isomers of both the mono and bi-metallic complexes **NdL$_a$** (Fig. 6c) and **Nd$_2$L$_b$** (Fig. 6e) were essentially identical (λ_{ex} = 580 nm), again confirming that photoswitching does not significantly perturb the crystal field of the Nd(III) complexes. Unlike in **EuL$_a$** and **Eu$_2$L$_b$**, for **NdL$_a$** and **Nd$_2$L$_b$** the most intense excitation band lies outside the region in which the azobenzene absorbs, and pleasingly, upon direct excitation into the $^4I_{9/2} \rightarrow {}^4G_{5/2}$, $^2G_{7/2}$ (λ_{ex} = 580 nm) band, we observed no change in the ratio of *E*/*Z* isomers in the PSS upon excitation (Fig. S60, ESI†).

As with **EuL$_a$** and **Eu$_2$L$_b$**, the azobenzene moiety does not act as an antenna in the Nd(III) complexes, revealed by the lack of contribution from the azobenzene ligands in the excitation spectra of both the *E* and *Z* isomers of **NdL$_a$** (Fig. 6b) and **Nd$_2$L$_b$** (Fig. 6d). Notably, previous reports have determined that the triplet (T_1) state of a tetra-*ortho*-flouro azobenzene resides around ~12 000 cm^{-1}.[80–82] This would suggest that there is sufficient spectral overlap of the azobenzene T_1 state with the excited states of Nd(III) (Fig. 7). However, the excitation spectra of the Nd(III)-azobenzene complexes reveal that no emission is observed upon excitation into the azobenzene core. We therefore propose that the lack of sensitisation in these systems is a result of inefficient energy transfer. Previous studies have reported that the rate of intersystem crossing between the S_1 and T_1 states is as fast as 10^{11} s^{-1} for azobenzenes.[83,84] We suggest that this intersystem crossing (ISC) is much faster than the rate of energy transfer from the T_1 state of the azobenzene ligand to the Nd(III) excited state, such that despite sufficient spectral overlap between T_1 and Nd(III), the excited Nd(III) states are not populated to a significant degree *via* the T_1 state of the ligand.[85]

We also observed no photoisomerisation of the azobenzene within the complex upon direct excitation into the Nd(III) metal centre (Fig. S60, ESI†), further supporting the notion that energy transfer between the metal centre and ligand is disfavoured. Overall, these experiments demonstrate that in the two

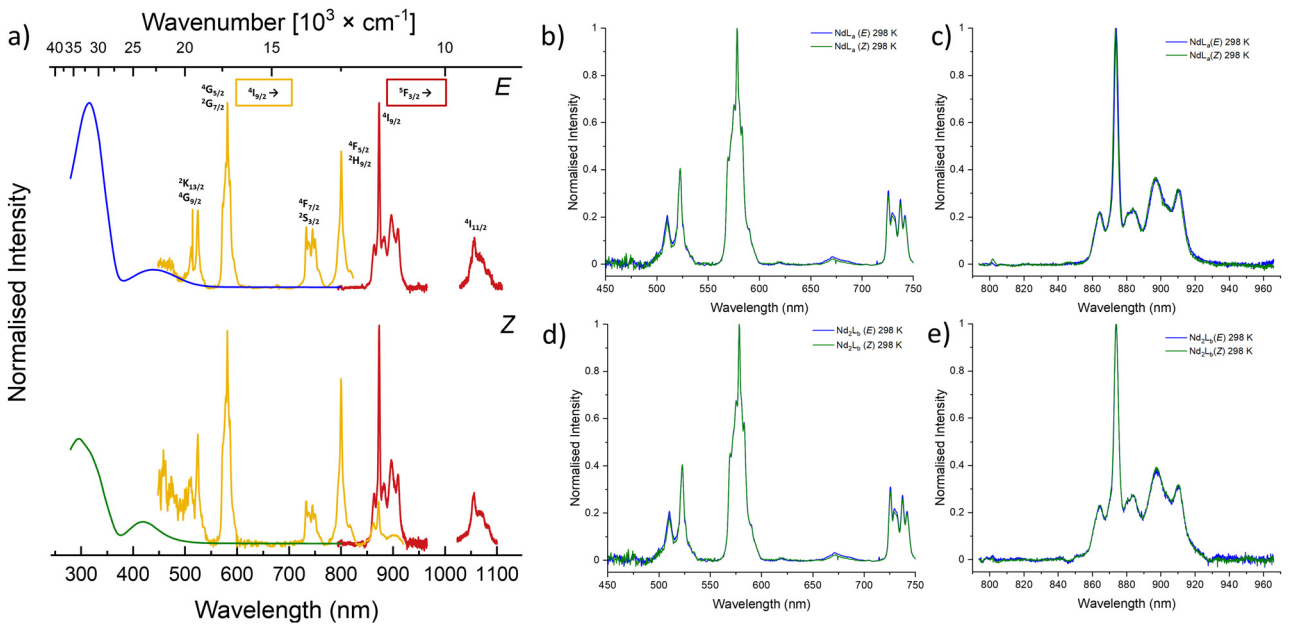

Fig. 6 (a) Stacked normalised spectra of **Nd$_2$L$_b$** (*E*) (above), and **Nd$_2$L$_b$** (*Z*) (below), with absorbance in blue (*E*) and green (*Z*), excitation spectra in yellow and emission spectra in red at 298 K. (b) Comparison of excitation spectra of **NdL$_a$** (*E*) (blue) and **NdL$_a$** (*Z*) (green) at 298 K. (c) Comparison of emission spectra of NdL$_a$ (*E*) (blue) and NdL$_a$ (*Z*) (green) at 298 K. (d) Comparison of excitation spectra of **Nd$_2$L$_b$** (*E*) (blue) and **Nd$_2$L$_b$** (*Z*) (green) at 298 K. (e) Comparison of emission spectra (λ_{ex} = 580 nm, emission slit at 25 μm) **Nd$_2$L$_b$** (*E*) (blue) and **Nd$_2$L$_b$** (*Z*) (green) at 298 K. Excitation spectra were recorded with λ_{em} = 880 nm, exposure time 100 ms, 1 exposure per frame. Emission spectra were recorded with λ_{ex} = 580 nm, emission slit at 25 μm corresponding to 1 nm spectral resolution. All spectra were recorded in DMSO.

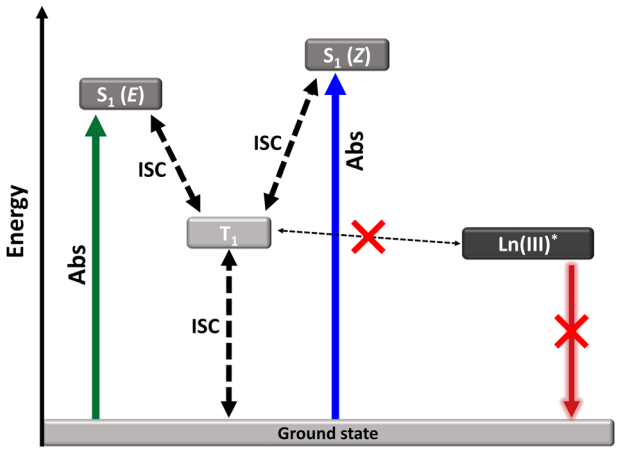

Fig. 7 Schematic diagram describing the dominating processes underpinning the photophysics of **NdL$_a$** and **Nd$_2$L$_b$**, dashed lines represent intersystem crossing (ISC), with bolded dashed lines representing the fast and dominant ISC between S_1 and T_1. Solid lines represent absorbance into the azobenzene S_1 states.

Nd(III) complexes the photoswitching process is completely independent and orthogonal to the photophysics of the Nd(III) metal centre, making these promising candidates for optical information storage.

Conclusions

We report the first examples of kinetically stable photoswitchable emissive lanthanide complexes in which the system can be controlled and interrogated by orthogonal wavelengths of visible and near-IR light. The mono and bi-metallic Eu(III) and Nd(III) photoswitchable complexes **EuL$_a$**, **Eu$_2$L$_b$**, **NdL$_a$** and **Nd$_2$L$_b$** display high photostationary state distributions when irradiated with orthogonal wavelengths of visible light (blue and green). Importantly, this photoswitching is entirely decoupled from the lanthanide excitation and emission, *i.e.* photoswitching does not sensitise lanthanide emission, while excitation of the lanthanide does not perturb the photostationary state distribution of the switch. This therefore represents an unprecedented fully orthogonal system, in which both visible light mediated switching and lanthanide excitation and emission are entirely independent, such that the system can be controlled and interrogated by four orthogonal wavelengths of light. This feature is requisite for applications in read/write optical information storage, and we anticipate that these results will pave the way for applications of such photoswitchable emissive complexes in this area, as well as more generally opening up new approaches to interrogating molecular photoswitchable devices by emission spectroscopy.

Author contributions

C. S. prepared and studied the compounds, V. N. and C. S. recorded Nd(III) spectra. All authors contributed to the analysis of the results. C. S. drafted the manuscript, with input and editing from all authors. S. F. and M. J. L conceived and supervised the project.

Data availability

The data supporting this article have been included as part of the ESI.†

Conflicts of interest

There are no conflicts to declare.

Acknowledgements

C. S. thanks the EPSRC Centre for Doctoral Training in Inorganic Chemistry for Future Manufacturing (OxICFM, EP/S023828/1) for studentship funding. V. R. M. N. thanks the DFF for studentship funding. We thank Carlsbergfondet and the Villum Foundation for support to build and acquires spectrometers. C. S thanks T. J. S for hosting 3-month research placement. C. S thanks M. J. L and S. F. for supervision and guidance. V. R. M. N. thanks T. J. S. for supervision and guidance. We thank Dr Aidan Kerckhoffs, Dr Toby Johnson, Dr Carlson Alexander and Dr Daniel Kovacs for useful discussion. M. J. L. is a Royal Society University Research Fellow.

References

1 M. Di Martino, L. Sessa, R. Diana, S. Piotto and S. Concilio, *Molecules*, 2023, **28**, 3712.
2 J. Yu, D. Qi and J. Li, *Commun. Chem.*, 2020, **3**, 189.
3 Y. L. Zhuang, X. L. Ren, X. T. Che, S. J. Liu, W. Huang and Q. Zhao, *Adv. Photonics*, 2021, **3**, 014001.
4 F. Xu and B. L. Feringa, *Adv. Mater.*, 2023, **35**, 2204413.
5 M. Clerc, S. Sandlass, O. Rifaie-Graham, J. A. Peterson, N. Bruns, J. Read De Alaniz and L. F. Boesel, *Chem. Soc. Rev.*, 2023, **52**, 8245–8294.
6 P. Kobauri, F. J. Dekker, W. Szymanski and B. L. Feringa, *Angew. Chem., Int. Ed.*, 2023, **62**, e202300681.
7 S. Crespi, N. A. Simeth and B. König, *Nat. Rev. Chem.*, 2019, **3**, 133–146.
8 J. Volarić, W. Szymanski, N. A. Simeth and B. L. Feringa, *Chem. Soc. Rev.*, 2021, **50**, 12377–12449.
9 D. H. Qu, Q. C. Wang, Q. W. Zhang, X. Ma and H. Tian, *Chem. Rev.*, 2015, **115**, 7543–7588.
10 A. Goulet-Hanssens, F. Eisenreich and S. Hecht, *Adv. Mater.*, 2020, **32**, 1905966.
11 E. R. Ruskowitz and C. A. Deforest, *Nat. Rev. Mater.*, 2018, **3**, 17087.
12 Y. Zhou, H. Ye, Y. B. Chen, R. Y. Zhu and L. C. Yin, *Biomacromolecules*, 2018, **19**, 1840–1857.
13 B. N. Sunil, W. S. Yam and G. Hegde, *RSC Adv*, 2019, **9**, 40588–40606.
14 E. Mitscherlich, *Ann. Pharm.*, 1834, **12**, 305–311.
15 A. A. Beharry and G. A. Woolley, *Chem. Soc. Rev.*, 2011, **40**, 4422.

16 A. Kerckhoffs and M. J. Langton, *Chem. Sci.*, 2020, **11**, 6325–6331.
17 A. Kerckhoffs, Z. Bo, S. E. Penty, F. Duarte and M. J. Langton, *Org. Biomol. Chem.*, 2021, **19**, 9058–9067.
18 M. Ahmad, S. Metya, A. Das and P. Talukdar, *Chem. – Eur. J.*, 2020, **26**, 8703–8708.
19 T. G. Johnson, A. Sadeghi-Kelishadi and M. J. Langton, *J. Am. Chem. Soc.*, 2022, **144**, 10455–10461.
20 Y. R. Choi, G. C. Kim, H.-G. Jeon, J. Park, W. Namkung and K.-S. Jeong, *Chem. Commun.*, 2014, **50**, 15305–15308.
21 W. A. Velema, W. Szymanski and B. L. Feringa, *J. Am. Chem. Soc.*, 2014, **136**, 2178–2191.
22 M. Wegener, M. J. Hansen, A. J. M. Driessen, W. Szymanski and B. L. Feringa, *J. Am. Chem. Soc.*, 2017, **139**, 17979–17986.
23 L. Josa-Culleré and A. Llebaria, *J. Med. Chem.*, 2023, **66**, 1909–1927.
24 M. Kapun, F. J. Pérez-Areales, N. Ashman, P. J. E. Rowling, T. Schober, E. Fowler, L. S. Itzhaki and D. R. Spring, *RSC Chem. Bio.*, 2024, **5**, 49–54.
25 T. Zhao, P. Wang, Q. Li, A. A. Al-Khalaf, W. N. Hozzein, F. Zhang, X. Li and D. Zhao, *Angew. Chem., Int. Ed.*, 2018, **57**, 2611–2615.
26 A. Díaz-Moscoso and P. Ballester, *Chem. Commun.*, 2017, **53**, 4635–4652.
27 T. Eom, W. Yoo, S. Kim and A. Khan, *Biomaterials*, 2018, **185**, 333–347.
28 F. Crick, *Philos. Trans. R Soc. Lond. B Biol. Sci.*, 1999, **354**, 2021–2025.
29 P. Hong, N.-H. Xie, K. Xiong, J. Liu, M.-Q. Zhu and C. Li, *J. Mater. Chem. A*, 2023, **11**, 5703–5713.
30 T. Nakagawa, Y. Hasegawa and T. Kawai, *Chem. Commun.*, 2009, 5630–5632.
31 M. M. Lerch, M. J. Hansen, W. A. Velema, W. Szymanski and B. L. Feringa, *Nat. Commun.*, 2016, **7**, 12054.
32 J. C. G. Bünzli and C. Piguet, *Chem. Soc. Rev.*, 2005, **34**, 1048–1077.
33 W. T. Carnall, P. R. Fields and K. Rajnak, *J. Chem. Phys.*, 1968, **49**, 4424–4442.
34 G. Marriott, R. M. Clegg, D. J. Arndtjovin and T. M. Jovin, *Biophys. J.*, 1991, **60**, 1374–1387.
35 M. C. Heffern, L. M. Matosziuk and T. J. Meade, *Chem. Rev.*, 2014, **114**, 4496–4539.
36 J. C. G. Bünzli and S. V. Eliseeva, *J. Rare Earths*, 2010, **28**, 824–842.
37 J. C. G. Bunzli, *Acc. Chem. Res.*, 2006, **39**, 53–61.
38 X. He, L. Norel, Y.-M. Hervault, R. Métivier, A. D'Aléo, O. Maury and S. Rigaut, *Inorg. Chem.*, 2016, **55**, 12635–12643.
39 H. B. Cheng, H. Y. Zhang and Y. Liu, *J. Am. Chem. Soc.*, 2013, **135**, 10190–10193.
40 H. Al Sabea, L. Norel, O. Galangau, T. Roisnel, O. Maury, F. Riobé and S. Rigaut, *Adv. Funct. Mater.*, 2020, **30**, 2002943.
41 H. Al Sabea, L. Norel, O. Galangau, H. Hijazi, R. Métivier, T. Roisnel, O. Maury, C. Bucher, F. Riobé and S. Rigaut, *J. Am. Chem. Soc.*, 2019, **141**, 20026–20030.
42 T. Nakagawa, Y. Hasegawa and T. Kawai, *J. Phys. Chem. A*, 2008, **112**, 5096–5103.
43 L.-R. Lin, X. Wang, G.-N. Wei, H.-H. Tang, H. Zhang and L.-H. Ma, *Dalton. Trans.*, 2016, **45**, 14954–14964.
44 L. R. Lin, H. H. Tang, Y. G. Wang, X. Wang, X. M. Fang and L. H. Ma, *Inorg. Chem.*, 2017, **56**, 3889–3900.
45 Y.-G. Wang, Y.-Q. Li, H.-H. Tang, L.-R. Lin and L.-H. Ma, *ACS Omega*, 2018, **3**, 5480–5490.
46 C.-Y. Fu, L. Chen, X. Wang and L.-R. Lin, *ACS Omega*, 2019, **4**, 15530–15538.
47 T. J. Sorensen and S. Faulkner, *Acc. Chem. Res.*, 2018, **51**, 2493–2501.
48 M. Cieslikiewicz-Bouet, S. V. Eliseeva, V. Aucagne, A. F. Delmas, I. Gillaizeau and S. Petoud, *RSC Adv.*, 2019, **9**, 1747–1751.
49 A. Guesdon-Vennerie, P. Couvreur, F. Ali, F. Pouzoulet, C. Roulin, I. Martínez-Rovira, G. Bernadat, F. X. Legrand, C. Bourgaux, C. L. Mazars, S. Marco, S. Trépout, S. Mura, S. Mériaux and G. Bort, *Nat. Commun.*, 2022, **13**, 4102–4114.
50 J. D. Routledge, X. J. Zhang, M. Connolly, M. Tropiano, O. A. Blackburn, A. M. Kenwright, P. D. Beer, S. Aldridge and S. Faulkner, *Angew. Chem., Int. Ed.*, 2017, **56**, 7783–7786.
51 T. J. Sørensen and S. Faulkner, *Acc. Chem. Res.*, 2018, **51**, 2493–2501.
52 M. H. V. Werts, R. T. F. Jukes and J. W. Verhoeven, *Phys. Chem. Chem. Phys.*, 2002, **4**, 1542–1548.
53 M. H. V. Werts, *Sci. Prog.*, 2005, **88**, 101–131.
54 N. Kofod, P. Nawrocki and T. J. Sorensen, *J. Phys. Chem. Lett.*, 2022, **13**, 3096–3104.
55 P. R. Nawrocki, N. Kofod, M. Juelsholt, K. M. Ø. Jensen and T. J. Sørensen, *Phys. Chem. Chem. Phys.*, 2020, **22**, 12794–12805.
56 K. Binnemans, *Coord. Chem. Rev.*, 2015, **295**, 1–45.
57 V. R. M. Nielsen, P. R. Nawrocki and T. J. Sorensen, *J. Phys. Chem. A*, 2023, **127**, 3577–3590.
58 P. R. Nawrocki and T. J. Sørensen, *Phys. Chem. Chem. Phys.*, 2023, **25**, 19300–19336.
59 P. R. Nawrocki, V. R. M. Nielsen and T. J. Sørensen, *Methods Appl. Fluoresc.*, 2022, **10**, 045007.
60 D. Bléger, J. Schwarz, A. M. Brouwer and S. Hecht, *J. Am. Chem. Soc.*, 2012, **134**, 20597–20600.
61 C. Knie, M. Utecht, F. L. Zhao, H. Kulla, S. Kovalenko, A. M. Brouwer, P. Saalfrank, S. Hecht and D. Bléger, *Chem. – Eur. J.*, 2014, **20**, 16492–16501.
62 A. Kerckhoffs, K. E. Christensen and M. J. Langton, *Chem. Sci.*, 2022, **13**, 11551–11559.
63 S. Samanta, A. A. Beharry, O. Sadovski, T. M. McCormick, A. Babalhavaeji, V. Tropepe and G. A. Woolley, *J. Am. Chem. Soc.*, 2013, **135**, 9777–9784.
64 M. Dong, A. Babalhavaeji, C. V. Collins, K. Jarrah, O. Sadovski, Q. Y. Dai and G. A. Woolley, *J. Am. Chem. Soc.*, 2017, **139**, 13483–13486.
65 Z. Ahmed, A. Siiskonen, M. Virkki and A. Priimagi, *Chem. Commun.*, 2017, **53**, 12520–12523.
66 A. Antoine John and Q. Lin, *J. Org. Chem.*, 2017, **82**, 9873–9876.

67 A. L. Leistner, S. Kirchner, J. Karcher, T. Bantle, M. L. Schulte, P. Gödtel, C. Fengler and Z. L. Pianowski, *Chem. – Eur. J.*, 2021, **27**, 8094–8099.
68 H. Satzger, S. Spörlein, C. Root, J. Wachtveitl, W. Zinth and P. Gilch, *Chem. Phys. Lett.*, 2003, **372**, 216–223.
69 W. T. Carnall, P. R. Fields and K. Rajnak, *J. Chem. Phys.*, 1968, **49**, 4450–4455.
70 T. Fujino, S. Y. Arzhantsev and T. Tahara, *J. Phys. Chem. A*, 2001, **105**, 8123–8129.
71 P. Bortolus and S. Monti, *Am. J. Phys. Chem.*, 1979, **83**, 648–652.
72 C. M. Stuart, R. R. Frontiera and R. A. Mathies, *J. Phys. Chem. A*, 2007, **111**, 12072–12080.
73 T. Fujino and T. Tahara, *J. Phys. Chem. A*, 2000, **104**, 4203–4210.
74 I. K. Lednev, T. Q. Ye, R. E. Hester and J. N. Moore, *Am. J. Phys. Chem.*, 1996, **100**, 13338–13341.
75 I. K. Lednev, T. Q. Ye, P. Matousek, M. Towrie, P. Foggi, F. V. R. Neuwahl, S. Umapathy, R. E. Hester and J. N. Moore, *Chem. Phys. Lett.*, 1998, **290**, 68–74.
76 K. J. Miller, A. A. Saherwala, B. C. Webber, Y. Wu, A. D. Sherry and M. Woods, *Inorg. Chem.*, 2010, **49**, 8662–8664.
77 G. Tircso, B. C. Webber, B. E. Kucera, V. G. Young and M. Woods, *Inorg. Chem.*, 2011, **50**, 7966–7979.
78 L. G. Nielsen and T. J. Sorensen, *Inorg. Chem.*, 2020, **59**, 94–105.
79 A. Beeby and S. Faulkner, *Chem. Phys. Lett.*, 1997, **266**, 116–122.
80 J. Isokuortti, K. Kuntze, M. Virkki, Z. Ahmed, E. Vuorimaa-Laukkanen, M. A. Filatov, A. Turshatov, T. Laaksonen, A. Priimagi and N. A. Durandin, *Chem. Sci.*, 2021, **12**, 7504–7509.
81 S. Monti, E. Gardini, P. Bortolus and E. Amouyal, *Chem. Phys. Lett.*, 1981, **77**, 115–119.
82 K. Kuntze, J. Viljakka, E. Titov, Z. Ahmed, E. Kalenius, P. Saalfrank and A. Priimagi, *Photochem. Photobio. Sci.*, 2022, **21**, 159–173.
83 E. R. Talaty and J. C. Fargo, *Chem. Commun.*, 1967, 65–66.
84 S. Axelrod, E. Shakhnovich and R. Gómez-Bombarelli, *ACS Cent. Sci.*, 2023, **9**(2), 166–167.
85 A. K. R. Junker, L. R. Hill, A. L. Thompson, S. Faulkner and T. J. Sorensen, *Dalton Trans.*, 2018, **47**, 4794–4803.